Metallomics

Accepted Manuscript

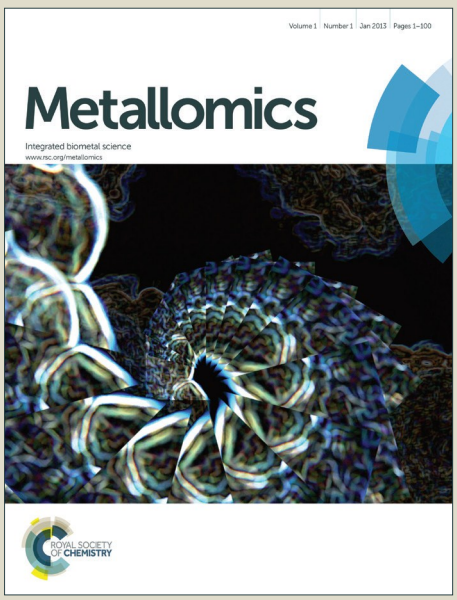

ROYAL SOCIETY OF CHEMISTRY

www.rsc.org/metallomics

IRON-DEPENDENT TURNOVER OF IRP-1/c-ACONITASE IN KIDNEY CELLS

Ying Liu and Douglas M. Templeton*

University of Toronto, Laboratory Medicine and Pathobiology

1 King's College Circle, Toronto, Ont., M5S 1A8, Canada

Running title: Iron-dependent IRP-1 degradation

*Address correspondence to:
Douglas M. Templeton
University of Toronto
Department of Laboratory Medicine and Pathobiology
1 King's College Circle
Toronto M5S 1A8, Canada.

Tel. 416-978-3972
Fax. 416-978-5959
e-mail: doug.templeton@utoronto.ca

ABSTRACT

The kidney plays an important role in iron homeostasis and actively reabsorbs citrate. The bifunctional iron-regulatory protein IRP-1 potentially regulates iron trafficking and participates in citrate metabolism as a cytosolic (c-) aconitase. We investigated the role of cellular iron status in determining the expression and dynamics of IRP-1 in two renal cell types, with the aim of identifying a role of the protein in cellular ROS levels, citrate metabolism and glutamate production. The effects of iron supplementation and chelation on IRP-1 protein and mRNA levels and protein turnover were compared in cultured primary rat mesangial cells and a porcine renal tubule cell line (LLC-PK1). Levels of ROS were measured in both cell types, and c-aconitase activity, glutamate, and glutathione were measured in LLC-PK1 cells, with and without IRP-1 silencing and in glutamine-supplemented or nominally glutamine-free medium. Iron supplementation decreased IRP-1 levels (e.g., approx. 40% in mesangial cells treated with 10 μg/ml iron for 16 h) and increased ubiquitinated IRP-1 levels in both cells types, with iron chelation having the opposite effect. Although iron increased ROS levels (three-fold with 20 μg/ml iron in mesangial cells and more modestly by about 30% with 50 μg/ml in LLC-PK1 cells, both after 24 h), protein degradation was not ROS-dependent. In LLC-PK1 cells, 10 μg/ml iron (24 h) increased both aconitase activity (30%) and secreted glutamate levels (65%). Silencing did not remove the glutamate response to iron but decreased the c-aconitase activity of the residual protein independent of iron loading (37% and 46% of control levels, without and with iron treatment, respectively). However, in glutamine-free medium, glutamate was still increased by iron, even in IRP-1-silenced cells, and did not correspond to c-aconitase. Silencing decreased the amount of ferritin measured in response iron loading, decreased the affect of iron on total glutathione by 48%, and increased the response of ROS to iron loading by 38%. We conclude that iron increases turnover of IRP-1 in kidney cells, while increasing aconitase activity, suggesting that the apoprotein (aconitase-inactive) form is not exclusively responsible for turnover. Iron increases glutamate levels in tubule epithelial cells, but this appears to be independent of c-aconitase activity or the availability of extracellular glutamine. IRP-1 protein levels are not regulated by ROS, but IRP-1-dependent ferritin expression may decrease ROS and

increase total glutathione levels, suggesting that ferritin levels are more important than citrate metabolism in protecting renal cells against iron.

Keywords: Iron regulatory protein; protein turnover; kidney cells; citrate; aconitase; iron metabolism.

Abbreviations:

AIP - apoptosis-inducing factor
BHA - butylated hydroxyanisole
DCF-DA - 2′,7′-dichlorodihydrofluorescein diacetate
DFO - deferoxamine
DTNB - 5,5′-dithio-*bis*-(2-nitrobenzoic acid)
EMSA - electromobility gel shift assay
FAC - ferric ammonium citrate
Ft - ferritin
GSH/GSSG - reduced/oxidzed glutathione
GAPDH - glyceraldehyde phosphate dehydrogenase
IRE - iron-responsive element
IRP - iron-regulatory protein
2-ME - 2 mercaptoethanol
RMC - rat mesangial cell
ROS - reactive oxygen species
RT-PCR - reverse transcription-polymerase chain reaction
TfR - transferrin receptor

1. INTRODUCTION

The kidney is an important organ regulating iron homeostasis. Current data support the model that transferrin-bound iron is filtered by the glomerulus and reabsorbed by the proximal tubules; the iron content of the proximal tubule correlates with the degree of tubular damage in iron-overloaded states [1]. Proximal tubule cells reabsorb 75 to 90% of the citrate that enters the glomerular filtrate. This reabsorbed citrate likely is metabolized to isocitrate by iron-dependent cytosolic (c-) aconitase, which can be metabolized further by cytosolic isocitrate dehygrogenase to yield 2-oxoglutarate/glutamate and NADPH, involved in defending against reactive oxygen species (ROS) [2].

Iron-regulatory protein-1 (IRP-1) regulates several proteins of iron metabolism by binding to iron-responsive elements (IRE) in their mRNAs, and is inactivated upon formation of an iron-sulfur [4Fe-4S] cluster that is required for c-aconitase activity [3]. Formerly the view that iron-dependent protein degradation played a lesser role than cluster assembly/disassembly in regulating RNA binding activity of IRP-1 was influenced by the observed preponderance of the c-aconitase form in immunoblots [3]. However, it is now established that the IRE-binding apo form of the protein is degraded by a proteasomal pathway [4-6]. IRP-1 is expressed at higher levels in kidney compared with other mouse tissues [7]. Animals that lack IRP-1 are unable to repress ferritin synthesis completely in the kidney under conditions of iron deficiency, demonstrating that IRP-1 contributes significantly to regulation of renal iron metabolism; in most other tissues, loss of IRP-1does not lead to dysregulation of iron metabolism [7]. We still do not fully understand the significance of abundant c-aconitase in cells.

We previously showed that IRP-1 undergoes iron-dependent down-regulation in rat renal mesangial cells (RMC) treated with iron following growth in low serum conditions [8]. Here we investigate this phenomenon further at the mRNA and protein levels, as a function of serum concentration, iron supplementation, and iron chelation. We also explore the mechanism of iron-dependent IRP-1 degradation in a proximal

tubule cell line (LLC-PK1) from pig kidney. RMC are compared in serum-starved (quiescent) cultures and under serum-replete conditions to assess the role of serum-depletion in earlier studies on IRP-1 metabolism. LLC-PK1 cells, a serum-dependent epithelial line, are studied under serum-replete conditions. The functional significance of IRP-1 as c-aconitase in LLC-PK1 is discussed. As IRP-1 is the predominant IRE-binding protein in kidney, whereas IRP-2 lacks aconitase activity and makes very little contribution to IRE-binding activity in kidney [9], IRP2 is not investigated here.

2. MATERIALS AND METHODS

2.1 *Cell culture:* Rat mesangial cells (RMC) were established as previously described [10]. Cells were cultured in RPMI-1640 medium with 10% FBS and used between passages 7 and 15. Overnight cultures were left in RPMI-1640 with 10% FBS or rendered quiescent in PRMI-1640 with 0.2% FBS for 24 h. Cells were treated with various concentration of ferric ammonium citrate (FAC) or 0.1 mM deferoxamine (DFO) for an additional 24 h in the corresponding media. LLC-PK1 cells were cultured in DMEM (1g/L glucose, 4 mM glutamine) with 10% FBS as described [11]. Overnight cultures were then treated with FAC or DFO for an additional 24 h. Some LLC-PK1 experiments were done in glutamine-free DMEM with 10% FBS. Both cell types were grown in a humidified atmosphere of 5% CO_2 at 37°C. In some experiments, cells were pre-treated with 50 μM butylated hydroxyanisole (BHA) for 1 h, then co-treated with FAC for 24 h. For proteasome inhibition studies, starved cells were pre-treated with 0.1 μM for MG-132 followed by FAC co-treatment for 24 h. For similar experiments in serum-replete medium, the MG-132 concentration was increased to 1μM.

2.2 *Cell fractionation:* Crude cytoplasmic extracts and subcellular fractions of purified cytosol were processed as described [8]. Briefly, cell pellets were lysed in extraction buffer (10 mM HEPES, pH 7.6, 3 mM $MgCl_2$, 40 mM KCl, 1 mM DTT with 0.2% Nonidet P-40 and protease inhibitors). After sonication twice for 5 sec, lysates were centrifuged at 10,000 x *g* for 10 min (4°C) and the supernatant was collected as crude cytoplasmic extract. Differential detergent fractionation was used to isolate a purer cytosolic fraction. First, cell pellets were resuspended in digitonin-sucrose buffer (5 mM Tris-HCl, pH 7.4, 250 mM sucrose, 1 mM EDTA, 1 mM EGTA, 1.5 mM $MgCl_2$, 0.007% digitonin and protease inhibitors) and incubated for 8 min on ice. Lysates were centrifuged at 1800 x *g* for 8 min (4°C), the supernatant was further centrifuged at 15,000 x *g* for 20 min (still at 4°C), and the second supernatant was taken as the cytosolic fraction. The pellets were resuspended and incubated with Trion X-100 buffer (20 mM Tris-HCl, pH 7.4, 2 mM $MgCl_2$, 138 mM KCl, 0.5% Triton X-100 with protease inhibitors) for 30 min on ice. The suspension was centrifuged at 8000 x g for 10 min

(4°C) and the supernatant was considered the membrane fraction. Purity of the cytosolic fraction was confirmed by the absence of the mitochondrial marker apoptosis inducing factor (AIF) and the membrane protein transferrin receptor (TfR); the membrane fraction was free of cytosolic marker glyceraldehyde phosphate dehydrogenase (GAPDH).

2.3 *siRNA experiments:* Predesigned and validated IRP-1 siRNA (cat#4390824-s671) and scramble control (cat#4390843) were purchased from AmBion (Life Technologies, Burlington, ON, Canada). The sequences for IRP-1 are:

5'→3', Sense: GCUCGCUACUUAACUAACAtt

Antisense: UGUUAGUUAAGUAGCGAGCag

$1x10^6$ LLC-PK1 was seeded in 60 mm plates and grown overnight. 10 nM of siRNA was transfected into cells using 8 μl of Lipofectamine RNAiMAX (Life Technologies) for 24 h as recommended by the manufacture. Cells were washed and treated with FAC or DFO for an additional 24 h. Silencing efficiency was confirmed by anti-AcoI Western blotting and aconitase activity measurement.

2.4 *Western blotting and immunoprecipitation:* Equal amount of proteins from subcellular fractions or total cell lysates were separated by 10% SDS-PAGE and transferred to nitrocellulose for immunoblotting. Antibody sources and dilution were as follows: Anti-AcoI (1:3500) from MyBioSource (San Diego, CA), anti-TfR (1:10,000) from Zymed (San Francisco, CA), anti-ferritin (1: 6000) and anti-β-actin (1:15000) from Sigma (St. Louis, MO), anti-ubiquitin (Ub_P4D1, 1:2000) from Santa Cruz Biotechnology (Santa Cruz, CA), and anti-GAPDH (1:5000) from Cell Signaling Technology (Danvers, MA). Crude cytoplasmic extract (250 μg) was immunoprecipitated using 1 μg of anti-AcoI antibody and the immune complex was pulled down with protein G agarose beads (Millipore, Billerica, MA). The bound proteins were separated by SDS/PAGE and probed with anti-AcoI and anti-ubiquitin. Enhanced chemiluminecent substrate (Amersham Bioscience, Baie d'Urfe, QC, Canada) was used for signal detection. Band density was quantified using Image J software (NIH, Bethesda, MD).

2.5 *Reverse transcriptase-polymerase chain reaction (RT-PCR):* Total RNA was extracted with an RNeasy kit according to instructions (Qiagen; Burlington, ON, Canada). Five μg total RNA was reverse transcribed with Minus M-MulV reverse transcriptase (Fermentas, Burlington, ON, Canada) with hexameric primer. IRP-1,TfR and actin mRNA transcripts were reverse transcribed and the products were amplified with primers as described [12]:

IRP-1:

(F) 5'-TTACCAAGCACCTCCGACAA-3'

(R) 5'-AATCCTGCGCCTAACATCA-3'

TfR:

(F) 5'-GGCCGGTCAGTTCATTATTA-3'

(R) 5'-CTCATGACGAATCTGTTGTT-3'

Actin:

(F) 5'-CTGAGGAGCACCCTGTGCTGCTC-3'

(R) 5'- CGGATGTCAACGTCACACTTCA -3'.

Reaction mixtures were heated to 94°C for 2 min and subsequent cycles were performed at three temperature steps of 94°C (30 s), 55°C (30 s), 72°C (45 s). A total of 30 cycles for IRP-1 and TfR and 25 cycles for actin were completed, followed by 72°C for 10 min for extension. Ethidium bromide-stained gels were scanned and quantified using Image J.

2.6 *Miscellaneous biochemical measurements:*

2.6.1 *ROS:* After treatment, cells were washed with PBS and incubated with 5 μM 2′,7′-dichlorodihydrofluorescein diacetate (H_2DCF-DA; Molecular Probes, Burlington, ON, Canada) in serum-free medium for 45 min at 37°C. Cells were trypsinized, washed and resuspended with 300 μl PBS. DCF fluorescence indicating the intracellular ROS level was analyzed in an Epics Elite flow cytometer (Beckman Coulter, Fullerton CA).

2.6.2 *Iron-regulatory element (IRE) electromobility gel shift assay (EMSA): In vitro* transcription and EMSA were performed as previously described [13]. Briefly, 1 μg linearized plasmid pSPTfer (coding human ferritin H-chain IRE) was labeled with α[^{32}P]CTP (800 Ci·mmol^{-1}; Perkin Elmer, Woodbridge, ON, Canada) using a Promega *in vitro* transcription system (Promega, Madison, WI). 10 μg of cell lysate was incubated

with a molar excess of labeled IRE (10 ng) in 10 mM HEPES pH 7.6, 3 mM $MgCl_2$, 40 mM KCl buffer. IRE–IRP complexes were resolved by 6% non-denaturing PAGE. Parallel samples were treated with 2% 2-mercaptoethanol before addition of the labeled probe to measure the total IRE binding activity.

2.6.3 *Aconitase activity:* Aconitase activity was determined by measuring the disappearance of aconitate absorbance 240 nm in buffer containing 50 mM Tris, pH 7.4, with 20 mM cis-aconitate and 50 μg of protein at room temperature as described [13]. Aconitase activity is reported as the amount of substrate converted in μmol/min/mg of protein.

2.6.4 *Glutamate:* Glutamate was measured using an Amplex Red glutamic acid/glutamate oxidase-based assay kit (Invitrogen, Burlington, ON, Canada) following the manufacturer's protocol as described [13]. Briefly, 50 μl conditioned media or 5 μg cell lysate was incubated with reaction buffer containing 100 μM Tris, pH 7.5, containing 50 μM Amplex Red, 0.125 U/ml horseradish peroxidase and 0.04 U/ml L-glutamate oxidase at 37°C for 30 min in the dark. Fluorescence was measured in a Fluostar Optima fluorescence microplate reader (BMG Labtech, Ortenberg, Germany) with excitation at 540 nm and emission at 590 nm.

2.6.5 *Total and reduced glutathione:* Glutathione (GSH) was measured using a 5,5′-dithio-*bis*-(2-nitrobenzoic acid) (DTNB) recycling assay as described [14]. Briefly, equal amounts of cell lysate were deproteinized using Deproteinizing Sample Preparation Kit (Biovision; San Francisco, CA.). Total glutathione (tGSH), was measured kinetically using a spectrophotometric microplate reader that involved oxidation of GSH by DTNB and recycling by glutathione reductase in the presence of NADPH for 2 min at room temperature. Oxidized glutathione (GSSG) was measured similarly after removing reduced GSH by addition of 1 M 2-vinylpyridine in 100% ethanol followed by triethanolamine to deproteinized samples.

2.7 *Statistical analysis:* Measured quantities are expressed as mean ± SD and significant differences were determined by one-way Anova with InStat software (Graph Pad, San

Diego, CA), using Dunnett's post hoc test for comparisons against a single control value, or the Tukey-Kramer test for multiple internal comparisons.

3. RESULTS

3.1 Rat mesangial cells

3.1.1 *Gene and protein expression:* To understand better the mechanism of iron-dependent down-regulation of IRP-1 in RMC, we investigated transcription, expression and degradation of IRP-1 after iron treatment. While serum deprivation (growth in 0.2% serum for 24 h prior to the experiment) renders RMC quiescent and facilitates studies in signaling and gene expression in the absence of growth factor-stimulated proliferation, this treatment itself exposes cells to decreased iron concentrations, and in this report we generally compare quiescent (serum-deprived) RMC with control RMC maintained continuously in 10% FBS. Compared to cells held in control conditions, deprived of serum, or treated with DFO, treatment with increasing concentrations of iron (from 5 to 20 μg/ml as FAC for 24 h) causes a decrease in total IRP-1 and TfR protein, and a concomitant increase in ferritin levels (Fig. 1A). This is consistent with the established ability of iron to decrease TfR and increase ferritin expression through regulation by IRP-1. Consistent with this, EMSA (Fig. 1B) shows that depleting iron either by serum deprivation (quiescent conditions) or DFO treatment increases IRP-1 binding activity. EMSA run after treatment with 2-mercaptoethanol (2-ME), generally considered to disrupt the 4Fe-4S cluster of the protein and facilitate maximum RNA binding, parallels EMSA without 2-ME treatment in quiescent cells. This supports the conclusion that a substantial decrease in iron availability (serum starvation with or without DFO) results in higher amounts of binding protein, although iron supplementation still decreases the binding. In control cells, with basal iron levels maintained by 10% serum, 2-ME does not reveal an effect of iron supplementation or DFO treatment, suggesting an effect on binding independent of changes in protein level when iron is not severely restricted.

IRP-1 mRNA steady-state levels were analyzed by reverse-transcription PCR. Modulating iron levels by treatment with DFO or addition of iron regulated TfR mRNA as expected; receptor transcript was decreased in higher iron in both quiescent and serum-replete cells and increased by iron chelation in serum-replete cells (Table 1). However,

IRP-1 mRNA levels remained relatively constant compared with a β-actin loading control, suggesting that transcription of IRP-1 is not affected by iron status, and the down-regulation of IRP-1 in RMC is instead through post-transcriptional regulation, possibly by inhibition of translation or increased IRP-1 turnover. Similar results were obtained in quiescent and control (serum-replete) cells (Table 1).

We then measured the effect of added iron (10 μg/ml as FAC) on IRP-1 in RMC as a function of time. IRP-1 is quite a stable protein with a half-life of more than 24 h, and its expression did not change with time in either quiescent cells without iron supplementation over 24 h (Fig. 2A) or in serum-replete medium up to 32 h (Fig. 2B). However, iron caused a decline in IRP-1 protein that reached a sustained decrease of approximately 40% by 16 h in low serum (Fig. 2A), and by 28-32 h in serum-replete growth medium (Fig. 2B). IRP-1 stability in RMC was further analyzed with the protein synthesis inhibitor cycloheximide (Fig. 2C, D). The protein level was not changed by cycloheximide (40 μM) alone up to 24 h in serum-replete medium. However, treatment of RMC with iron in the presence of cycloheximide decreased the IRP-1 level with a $t_{1/2}$ ~ 6-8 h in quiescent cells (low-iron medium) and 16-20 h in serum-replete conditions, suggesting iron increases IRP-1 turnover.

In eukaryotes, two major proteolytic systems are involved in degradation of denatured proteins, the lysosomes and the ubiquitin-proteasome machinery. Both pathways have been shown to be involved in IRP-2 degradation [15, 16], and apo-IRP-1 (without the [4Fe-4S] cluster) is degraded by the ubiquitin-proteasome pathway [4, 6, 17]. In quiescent cells in the presence of FAC, expression of IRP-1 (Fig. 3A) was significantly reduced ($p<0.01$, $n=4$). However, the proteasomal inhibitor MG-132 (0.1 μM) prevented an iron-dependent decrease in IRP-1. Similarly, in serum-replete growth medium (Fig. 3B), iron treatment alone at 10 μg/ml significantly decreased IRP-1 protein ($p<0.05$, $n=6$), and MG-132 (1 μM) again resulted in higher IRP-1 levels in iron-treated cells compared to iron treatment in the absence of inhibitor. Thus, in both serum-starved and serum-replete cells, the proteasomal pathway appears to be necessary for iron-dependent degradation of IRP-1.

Immunoprecipitation and immunoblotting were performed to determine whether IRP-1 was ubiquitinated. There was a decrease in IRP-1 in both immunoprecipitates and total lysates from iron-treated cells, compared to untreated or DFO-treated cells (Fig. 4). Immunoprecipitates of IRP-1 from iron-treated cells showed increased levels of ubiquitination compared to untreated or DFO-treated cells. TfR, an internal control in these experiments, was decreased in total lysates of the iron-treated cells, consistent with Fig. 1A and Table 1. These results were found for both quiescent and serum-replete cells.

3.1.2 *ROS involvement:* Previous studies showed that oxidative damage can increase the proteolytic susceptibility of m-aconitase [18] and IRP-1 [19], and extensive oxidation causes aggregation of m-aconitase protein [18]. ROS levels markedly increased after 10 μg/ml iron treatment [(316 ± 38)%, n=3, $p<0.001$], and BHA significantly decreased ROS [(30 ± 3)%, n=2] compared to control levels in quiescent cells. However, co-treatment with BHA and iron had no effect on iron-dependent IRP-1 degradation (Supplementary Fig. 1), suggesting that iron-dependent degradation of IRP-1 in RMC is independent of ROS.

3.2 Proximal tubule cells

3.2.1 *Protein expression and degradation:* We next examined whether the iron-dependent degradation of IRP-1 observed in RMC also occurred in serum-replete LLC-PK1 cells, a pig kidney proximal tubule cell line that was shown to be sensitive to ferric and ferrous citrate treatment [20]. IRP-1 and TfR are highly expressed in the proximal tubule, reflecting the importance of this structure in iron regulation [2]. Iron at 5 μg/ml or more down-regulated IRP-1 in LLC-PK1 cells, and DFO increased it slightly (Fig. 5A), as seen in RMC. Again, TfR and ferritin were regulated by iron status, in the directions expected. The decrease in IRP-1 protein level was reversed by co-treatment with the proteasomal inhibitor MG-132 (Fig. 5B). The ubiquitin-proteasome pathway was further confirmed to be involved by IRP-1 immunoprecipitation, which showed that

iron increased IRP-1 ubiquitination (Fig. 5C). In contrast to RMC, in which iron at 5-20 μg/ml increased ROS two- to three-fold in serum-replete cells, iron did not increase ROS significantly until 50 μg/ml in LLC-PK1 cells, and then the increase was only about 30% (Fig. 6). And, DFO also increased ROS in LLC-PK1 cells, by about 20% compared with untreated control. These results further confirm that iron-dependent degradation in both RMC and LLC-PK1 is not dependent upon ROS generation. They also suggest that LLC-PK1 cells are more resistant to iron loading than RMC.

3.2.2 IRP-1 gene silencing: In order to explore a functional link between c-aconitase and cytosolic glutamate, IRP-1 expression was silenced and the effect of this knock-down on IRP-1 expression was determined. As expected, IRP-1 was decreased in the silenced cells and was unresponsive to iron manipulation (Fig. 7). The basal level of TfR protein was lower in IRP-1 knock-down cells, consistent with less IRE binding activity of IRP-1. On the other hand, ferritin was not increased by IRP-1 silencing, suggesting that residual IRE binding activity is sufficient to repress ferritin synthesis under basal conditions. Control cells showed an increase in ferritin protein and a decrease in TfR protein in response to iron, and DFO increased TfR expression as expected (Fig. 7). In IRP-1-silenced cells, the increase in ferritin by iron loading and the increase in TfR by DFO were less prominent than the changes in the corresponding control cells. These results indicate the responses of ferritin and TfR to iron and DFO are partially impaired by IRP-1 silencing, consistent with IRP-1 being the predominant IRE-binding protein in kidney cells [7].

3.2.3 *Aconitase and glutamate levels:* Because IRP-1 exists predominantly as c-aconitase in the kidney [2], we wondered whether the down-regulation of IRP-1 at the protein level in LLC-PK1 cells has an impact on aconitase activity and cellular glutamate levels. A cytosolic fraction isolated by differential detergent fractionation as previously described [13] had decreased IRP-1 levels after FAC treatment (Fig. 8A), while c-aconitase activity was significantly increased by iron loading and inhibited by DFO treatment (Fig. 8B), as has been reported for other cell types [21,22]. A corresponding iron-dependent down-regulation of membrane-associated TfR was observed (Fig. 8A). Cytosolic glutamate

levels (Fig. 8C) trended with c-aconitase activity, being increased by FAC treatment and decreased by iron chelation, as reported in retinal pigment epithelial cells [22].

In siRNA silencing experiments, cytosolic glutamate levels increased in both IRP-1-silenced control cells and silenced FAC-treated cells, compared with unsilenced control cells (Table 2, 3rd column). They also differed significantly from the corresponding DFO-treated cells (Table 2, 4th column). Iron increased c-aconitase activity in random-sequence transfected control cells [(159 ± 38)% vs. no added iron (n=5)], whereas silencing decreased c-aconitase activity to a similar extent independent of iron supplementation [(37 ± 18)% and (46 ± 27)% of untreated control without or with iron treatment, respectively (n=5)]. Because chelation with DFO nearly eliminated aconitase activity (Fig. 8B), the activity was not measured following DFO treatment in this or the following experiments.

3.2.4 *Silencing in nominally glutamine-free medium:* The silencing experiments above were done in DMEM with 4 mM glutamine added to the growth medium, and we wondered whether glutamine uptake and conversion to cytosolic glutamate could confound the apparent changes caused by manipulating c-aconitase levels. Therefore, we repeated these experiments in DMEM without glutamine supplementation. Glutamate secretion (i.e., glutamate concentration measured in conditioned glutamine-free medium) was increased to the same extent by iron in both control and IRP-1-silenced cells (Table 3).

Cytosolic glutamate concentration was increased by iron in samples from silenced cells [(168 ± 32)%] compared with both control (100%) and DFO-treated samples [(102 ± 30)%]. Glutamate from total cell lysates in both control and iron-treated silenced samples was increased compared with control and DFO-treated cells, although again there was an almost 50% decrease in c-aconitase activity in silenced cells (data not shown). c-Aconitase activity in control cells grown in glutamine-free medium was comparable to that of control cells in glutamine-supplemented medium (Table 4). However, iron did not increase c-aconitase activity in glutamine-free medium. Taken

together, these results suggest the iron-dependent increases in glutamate are not correlated with c-aconitase activity.

3.2.5 *Glutathione levels after IRP-1 silencing:* Increased cellular ferritin has been shown to decrease ROS accumulation and protect cells against oxidative stress [23, 24], whereas a decrease in ferritin levels induced by TGF-β in AML-12 cells increased an intracellular labile iron pool and promoted ROS formation [25]. ROS levels were increased in IRP-1-silenced LLC-PK1 cells compared with the corresponding negative siRNA controls (Fig. 9A). This accompanies a decrease of [(31 ± 12)%, n=5] in total glutathione concentration in whole lysates of silenced cells compared with the negative siRNA controls, while the ratio of reduced-to-oxidized glutathione is unchanged [(7.0 ± 1.2) in control vs. (6.4 ± 1.4) in silenced]). However, in the cytosolic fraction, tGSH in silenced cells is comparable to tGSH in negative siRNA controls, and iron treatment decreases tGSH in both (Fig.9B). On the other hand, DFO appears to increase cytosolic tGSH in both silenced and control cells, although this only reaches significance in the controls. The compromised ability to increase ferritin expression may partially explain the increase in ROS in silenced cells.

4. DISCUSSION

Protein stability appears to be an important feature of IRP-1 regulation. IRP-1 can generally be considered a stable protein, with a half-life of more than 24 h irrespective of iron levels and physiological state [17, 26]. However, a few studies have demonstrated an iron-sensitive regulation. Goessling et al. [27] first showed that IRP-1 was down-regulated by iron in a normal rabbit skin fibroblast line (RAB-9). A marked decrease in IRP-1 expression in human liver was observed in patients with iron overload due to hereditary haemochromatosis type 1 [28]. Other studies have demonstrated that IRP-1 can be degraded in conditions of increased iron concentration when iron-sulfur cluster assembly is impaired, such as occurs with mutation of cluster-ligating cysteines, disruption of iron-sulfur cluster biogenesis, or destabilization of the cluster by IRP-1 phosphorylation [4, 17]. Upon overexpression of IRP-1 by transfection, the apoprotien is degraded under conditions of iron loading through a ubiquitin-proteasome pathway, probably involving F-box and leucine-rich repeat protein 5 (FBXL5) E3 ubiquitin ligase [5, 6]. The contribution of protein degradation to regulation of IRP-1 *in vivo* is not completely understood, although it has been suggested that iron-mediated IRP-1 degradation is a compensatory mechanism to eliminate excess IRE binding activity when apoIRP-1 cannot switch to c-aconitase forms (reviewed in [3]).

Serum deprivation is a physiological means of increasing the proportion of IRP-1 in the apoprotein form, and we previously showed that IRP-1 undergoes iron-dependent down-regulation in RMC cultured in iron-starvation conditions (48 h starvation in 0.2% FBS, followed by an additional 6 h iron treatment in serum-free medium [8]. In the present study serum starvation is again shown to increase IRP-1 protein degradation in renal cells. However, degradation of IRP-1 was also observed in RMC grown in medium containing 10% FBS. The level of IRP-1 protein is not affected by iron in many cell types, including HepG2 [29, 30], HEK-293 [31], rat hepatoma FTO2B and HeLa [32] grown in 10% FBS, and it has been suggested that this is a consequence of the more stable c-aconitase form masking changes in the less abundant apoprotein [3]. However, , the majority (perhaps more than 80%) of IRP1 in kidney is not in the IRE-binding form, with 60% showing c-aconitase activity [7]. The observation in the present study of iron-

dependent degradation in both RMC and LLC-PK1 cells grown in serum-replete medium may indicate that with the high abundance of IRP-1 in kidney cells [7], other forms of IRP-1 also become sensitive to iron-induced degradation as another compensatory mechanism to prevent excess IRE binding activity. Although total IRP-1 protein is decreased, c-aconitase activity is increased by iron, in agreement with earlier observations [3].

The function of c-aconitase is unclear. Narahari et al. [33] expressed IRP-1 in mitochondrial (m-) aconitase-deficient yeast (*aco1*) to demonstrate that the c-aconitase activity of IRP-1 can partially replace m-aconitase activity and rescue *aco1* from glutamate auxotrophy. Another yeast strain with a double mutation in m-aconitase and NADP-dependent isocitrate dehydrogenese expresses increased c-aconitase activity and exhibits growth similar to wild type in glutamate-free media [33]. The authors further propose that c-aconitase plays a role in fatty acid metabolism and the 2-oxoglutarate/glutamate synthesis pathway. Iron was shown to increase c-aconitase activity and lead to enhanced glutamate synthesis and secretion in glutaminergic retinal pigment epithelial cells[22], and increased glutathione levels in response to iron in these cells was due to c-aconitase-dependent glutamate synthesis [34]. However, a functional link between c-aconitase, glutamate and glutathione was proposed on the basis of experiments using an iron chelator (dipyridyl) and an aconitase inhibitor (oxalomalate), so a contribution from m-aconitase cannot be ruled out. Cell density has been shown influence switching of IRP-1 between its two functions [13]. High density cultures of several cell types, including hepatocytes and RMC have higher c-aconitase activity and cellular glutamate levels compared with low density cultures [13]. Cytosolic glutamate and the ratio of reduced to oxidized glutathione were both increased in higher density hepatocyte cultures [13]. Glutamate is a precursor and NADPH is a co-factor for synthesis of glutathione. Thus, the by-products NADPH and glutathione are both potentially made available for a role in defense against iron-mediated oxidative stress.

This model has not been tested yet in kidney cells. The proximal tubule absorbs up to 90% of the citrate in the glomerular filtrate [35]. This reabsorbed citrate may be

metabolized by c-aconitase into 2-oxoglutarate/glutamate; otherwise increased citrate might inhibit glycolysis and the citrate-iron complex might become toxic [2, 7]. From the present study, we can conclude that both mesangial and proximal tubule cell lines show increased ubiquitination and turnover of IRP-1 in response to iron, with the proximal tubule cells showing increases in both c-aconitase and cytosolic glutamate upon iron exposure and, conversely, decreases upon iron chelation. The iron-dependent increase in glutamate was also observed with cells grown in glutamine-free medium, although under these conditions it was not associated with an increase in c-aconitase activity, indicating additional sources of glutamate production in glutamine-deprived cells. Silencing IRP-1 was associated with an increase in ROS that could account for a decrease in total cellular glutathione. Thus, iron increases c-aconitase and glutamate levels in the proximal tubule cells, despite increasing proteasomal turnover of total IRP-1 protein, indicating that the level of this activity is not solely dependent on protein levels. Furthermore, the resultant glutamate does not appear to serve to increase glutathione defenses. Rather, the iron-dependent lowering of citrate may protect the cells from toxic levels of ferric citrate, as has been suggested [7]. This may also reflect IRP-1-dependent ferritin expression that decreases ROS and increases total glutathione levels, suggesting an important role of ferritin in conjunction with decreased citrate to protect renal cells from iron.

ACKNOWLEDGMENTS

Supported by an operating grant from the Natural Sciences and Engineering Research Council of Canada.

REFERENCES

1. C. P. Smith and F. Thévenod, Iron transport and the kidney. *Biochim. Biophys. Acta*, 2009, **1790**, 724-730.
2. D. Zhang, E. Meyron-Holtz and T. A. Rouault, Renal iron metabolism: transferrin iron delivery and the role of iron regulatory proteins. *J. Am. Soc. Nephrol.*, 2007, **18**, 401-406.
3. C. P. Anderson, M. Shen, R. S. Eisenstein and E. A. Leibold, Mammalian iron metabolism and its control by iron regulatory proteins. *Biochim. Biophys. Acta*, 2012, **1823**, 1468-1483.
4. J. Wang, C. Fillebeen, G. Chen, A. Biederbick, R. Lill and K. Pantopoulos, Iron-dependent degradation of apo-IRP1 by the ubiquitin-proteasome pathway. *Mol. Cell. Biol.*, 2007, **27**, 2423-2430.
5. A. A. Salahudeen, J. W. Thompson, J. C. Ruiz, H.-W. Ma, L. N. Kinch, Q. Li, N. V. Grishin and R. K. Bruick, An E3 ligase possessing an iron-responsive hemerythrin domain is a regulator of iron homeostasis. *Science*, 2009, **326**, 722-726.
6. A. A. Vashisht, K. B. Zumbrennen, X. Huang, D. N. Powers, A. Durazo, D. Sun, N. Bhaskaran, A. Persson, M. Uhlen, O. Sangfelt, C. Spruck, E. A. Leibold and J. A. Wohlschlegel, Control of iron homeostasis by an iron-regulated ubiquitin ligase. *Science*, 2009, **326**, 718-721.
7. E. G. Meyron-Holtz, M. C. Ghosh, K. Iwai, T. LaVaute, X. Brazzolotto, U. V. Berger, W. Land, H. Ollivierre-Wilson, A. Grinberg, P. Love and T. A. Rouault, Genetic ablations of iron regulatory proteins 1 and 2 reveal why iron regulatory protein 2 dominates iron homeostasis. *EMBO J.*, 2004, **23**, 386-395.
8. Y. Liu, W. Xiao and D. M. Templeton, Cadmium-induced aggregation of iron regulatory protein-1. *Toxicology*, 2014, **324**, 108-115.
9. M. C. Ghosh, D.-L. Zhang, S. Y. Jeong, G. Kovtunovych, H. Ollivierre-Wilson, A. Noguchi, T. Tu, T. Senecal, G. Robinson, D. R. Crooks, W.-H. Tong, K. Ramaswamy, A. Singh, B. B. Graham, R. M. Tuder, Z.-X. Yu, M. Eckhaus, J. Lee, D. A. Springer and T. A. Rouault, Deletion of iron regulatory protein 1 causes polycythemia and pulmonary hypertension in mice through translational derepression of HIF2. *Cell Metab.*, 2013, **17**, 271-281.
10. Z. Wang, T. A. Chin and D. M. Templeton, Calcium-independent effects of cadmium on actin assembly in mesangial and vascular smooth muscle cells. *Cell Motil. Cytoskeleton*, 1996, **33**, 208-222.
11. D. M. Templeton, Cadmium uptake by cells of renal origin. *J. Biol. Chem.*, 1990, **265**, 21764-21770.

12. H. Xu, H. Jiang, J. Wang and J. Xie, Rg1 protects iron-induced neurotoxicity through antioxidant and iron regulatory proteins in 6-OHDA-treated MES23.5 cells. *J. Cell. Biochem.*, 2010, **111**, 1537-1545.

13. Z. Popovic and D. M. Templeton, Cell density-dependent shift in activity of iron regulatory protein 1 (IRP-1)/cytosolic (c-)aconitase. *Metallomics*, 2012, **4**, 693-699.

14. G. Choong, Y. Liu, W. Xiao and D. M. Templeton, Cadmium-induced glutathionylation of actin occurs through a ROS-independent mechanism: implications for cytoskeletal integrity. *Toxicol. Appl. Pharmacol.*, 2013, **272**, 423-430.

15. A. H. Chang, J. Jeong and R. L. Levine, Iron regulatory protein 2 turnover through a nonproteasomal pathway. *J. Biol. Chem.*, 2011, **286**, 23698-23707.

16. T. Moroishi, T. Yamauchi, M. Nishiyama and K. I. Nkayama, HERC2 targets the iron regulator FBXL5 for degradation and modulates iron metabolism. *J. Biol. Chem.*, 2014, **289**, 16430-16441.

17. S. L. Clarke, A. Vasanthakumar, S. A. Anderson, C. Pondarre, C. M. Koh, K. M. Deck, J. S. Pitula, C. J. Epstein, M. D. Fleming and R. S. Eisenstein, Iron-responsive degradation of iron-regulatory protein 1 does not require the Fe-S cluster. *EMBO J.*, 2006, **25**, 544-553.

18. D. A. Bota and K. J. Davies, Lon protease preferentially degrades oxidized mitochondrial aconitase by an ATP-stimulated mechanism. *Nature Cell Biol.*, 2002, **4**, 674-680.

19. R. R. Starzynski, P. Lipinski, J.-C. Drapier, A. Diet, E. Smuda, T. Bartlomiejczyk, M. A. Gralak and M. Kruszewski, Down-regulation of iron regulatory protein 1 activities and expression in superoxide dismutase 1 knock-out mice is not associated with alterations in iron metabolism. *J. Biol. Chem.*, 2005, **280**, 4207-4212.

20. H. T. Sponsel, A. C. Alfrey, W. S. Hammond, J. A. Durr, C. Ray and R. J. Anderson, Effect of iron on renal tubular epithelial cells. *Kidney Int.*, 1996, **50**, 436-444.

21. B. L. Gourley, S. B. Parker, B. J. Jones, K. B. Zumbrennen and E. A. Leibold, Cytosolic aconitase and ferritin are regulated by iron in Caenorhabditis elegans. *J. Biol. Chem.*, 2003, **278**, 3227-3234.

22. M. C. McGahan, J. Harned, M. Mukunnemkeril, M. Goralska, L. Fleisher and J. B. Ferrell, Iron alters glutamate secretion by regulating cytosolic aconitase activity. *Am. J. Physiol.*, 2005, **288**, C1117-C1124.

23. K. Orino, L. Lehman, Y. Tsuji, H. Ayaki, S. V. Torti and F. M. Torti, Ferritin and the response to oxidative stress. *Biochem. J.*, 2001, **357**, 241-247.

24. K. J. Haro, A. Sheth and D. A. Scheinberg, Dysregulation of IRP1-mediated iron metabolism causes gamma ray-specific radioresistance in leukemia cells. *PLoS ONE*, 2012, **7**, e48841.

25. K.-H. Zhang, H.-Y. Tian, X. Gao, W.-W. Lei, Y. Hu, D.-M. Wang, X.-C. Pan, M.-L. Yu, G.-J. Xu, F.-K. Zhao and J.-G. Song, Ferritin heavy chain-mediated iron homeostasis and subsequent increased reactive oxygen species production are essential for epithelial-mesenchymal transition. *Cancer Res.*, 2009, **69**, 5340-5348.

26. C. K. Tang, J. Chin, J. B. Harford, R. D. Klausner and T. A. Rouault, Iron regulates the activity of the iron-responsive element binding protein without changing its rate of synthesis or degradation. *J. Biol. Chem.*, 1992, **267**, 24466-24470.

27. L. S. Goessling, D. P. Mascotti, M. Bhattacharyya-Pakrasi, H. Gang and R. E. Thach, Irreversible steps in the ferritin synthesis induction pathway. *J. Biol. Chem.*, 1994, **269**, 4343-4348.

28. M. Neonaki, G. Cunninghame, K. White and A. Bomford, Down-regulation of liver iron-regulatory protein I in haemochromatosis. *Biochem. Soc. Trans.*, 2002, **30**, 726-728.

29. Z. Popovic and D. M. Templeton, Iron accumulation and iron-regulatory protein activity in human hepatoma (HepG2) cells. *Mol. Cell. Biochem.*, 2004, **265**, 37-45.

30. Z. Popovic and D. M. Templeton, Inhibition of an iron-responsive element/iron regulatory protein-1 complex by ATP binding and hydrolysis. *FEBS J.*, 2007, **274**, 3108-3119.

31. C. Fillebeen, A. Caltagirone, A. Martelli, J.-M. Moulis and K. Pantopoulos, IRP1 Ser-711 is a phosphorylation site, critical for regulation of RNA-binding and aconitase activities. *Biochem. J.*, 2005, **388**, 143-150.

32. B. Guo, J. D. Phillips, Y. Yu and E. A. Leibold, Iron regulates the intracellular degradation of iron regulatory protein 2 by the proteasome. *J. Biol. Chem.*, 1995, **270**, 21645-21651.

33. J. Narahari, R. Ma, M. Wang and W. E. Walden, The aconitase function of iron regulatory protein 1. Genetic studies in yeast implicate its role in iron-mediated redox regulation. *J. Biol. Chem.*, 2000, **275**, 16227-16234.

34. M. M. Lall, J. Ferrell, S. Nagar, L. N. Fleisher and M. C. McGahan, Iron regulates L-cystine uptake and glutathione levels in lens epithelial and retinal pigment epithelial cells by its effect on cytosolic aconitase. *Invest. Ophthalmol. Vis. Sci.*, 2008, **49**, 310-319.

35. O. W. Moe and P. A. Preisig, Dual role of citrate in mammalian urine. *Curr. Opin. Nephrol. Hypertens.*, 2006, **15**, 419-424.

Table 1: Effect of iron status on TfR and IRP-1 mRNA levels in RMC.

Conditions	TfR (%)	IRP-1 (%)
Quiescent	100	100
+ DFO	99 ± 20	88 ± 28
+ Fe (10 μg/ml)	11 ± 3 **	111 ± 24
Serum-replete	100	100
+ DFO	179 ± 29 *	88 ± 8
+ Fe (10 μg/ml)	28 ± 6 *	94 ± 15

Cells grown for 24 h in 0.2% FBS (quiescent) or continuously in 10% FBS (serum-replete) were then treated with either 0.1 mM DFO for 24 h or supplemented with iron (10 μg/ml as FAC) for 24 h, and RNA was reverse-transcribed for PCR analysis. Values are mean ± SD, n=3. Differs from the corresponding quiescent value at $p < 0.001$ (**) or from the serum control at $p < 0.01$ (*). Other values are not significantly different from 100%.

Table 2: Cytosolic glutamate concentrations in control and IRP-1-silenced LLC-PK1 cells.

Treatment	Glutamate	P vs. control	P vs. DFO
Control	100	–	NS
+ DFO	84 ± 13	NS	–
+ Fe	108 ± 9	NS	< 0.05
Silenced	124 ± 21	< 0.05	< 0.001
+ DFO	103 ± 12	NS	NS
+ Fe	130 ± 20	< 0.01	< 0.001

Control cells were transfected with scrambled sequence. Transfections (control or silencing) were for 24 h followed by 24 treatment with either 0.1 mM DFO or FAC (10 µg/ml iron). Values are% of that measured in untreated control cells, mean ± SD, n=7. NS, not significant.

Table 3: Glutamate secretion into glutamine-free medium by control and IRP-1 gene-silenced LLC-PK1cells.

Treatment	Glutamate	P vs. Control	P vs. Silenced
Control	100	–	NS
+ DFO	69 ± 7	NS	NS
+ Fe	165 ± 39	<0.01	<0.001
Silenced	82 ± 7	NS	–
+ DFO	67 ± 12	NS	NS
+ Fe	148 ± 23	<0.05	<0.01

Medium was collected for glutamate analysis 48 h after transfection, immediately after 24 h treatment with either 0.1 mM DFO or FAC (10 μg/ml iron). Values are% of that measured in untreated control transfected cells, mean ± SD, n=4. NS, not significant.

Table 4: Effect of iron on c-aconitase activity in LLC-PK1 cells grown with or without glutamine supplementation.

Treatment	Aconitase activity (%)	P vs. (+ Gln, Control)	P vs. (+ Gln, Fe)
+ Gln, Control	100	_	< 0.05
+ Gln, Fe (10 µg/ml)	130 ± 21	< 0.05	–
- Gln, Control	96 ± 8	NS	< 0.05
- Gln, Fe (10 µg/ml)	74 ± 22	NS	< 0.001

Cells were grown in medium with or without glutamine for 24 h and then treated in the same medium with FAC (10 µg/ml iron) for an additional 24 h. Values are mean ± SD, n=5.

FIGURE LEGENDS

Fig.1 - Effect of iron loading and chelation on IRP-1 protein levels and IRE-binding activity in mesangial cells. **A)** Western blots of IRP-1, transferrin receptor (TfR), ferritin (Ft) and β-actin as a loading control are shown with extracts of mesangial cells grown in 10% FBS (first five lanes) or 0.2% FBS (next 5 lanes). Control cells (C) proliferating in 10% serum or quiescent cells (Q) in 0.2% serum were treated with 0.1 mM DFO (D) or iron at the indicated concentrations (as FAC). **B)** Control (C) or Quiescent (Q) cells in 10% or 0.2% serum as in A) were treated with DFO (D) or iron as indicated. EMSA was performed as described in Methods (Section 2.6.2) with (bottom panel) or without (top panel) 2-mercaptorethanol (2-ME). The fainter top band is at the position of the loading wells and the arrows indicate the retarded probe.

Fig. 2 - Effect of iron on IRP-1 turnover in mesangial cells. Representative Western blots are shown in all panels, of IRP-1 or β-actin loading control in total cell lysates, and the results of quantitation by densitometry are shown in the panel immediately below each blot (filled circles - 10 μg/ml iron as FAC for the indicated time; open circles - parallel cultures with no added iron for the corresponding times), taking the value at time = 0 as 100% **A)** Quiescent cells grown in 0.2% serum. **B)** Cells grown in 10% serum. **C)** Quiescent cells grown in 40 μM cycloheximide from time = 0. **D)** Cells grown in 10% serum with 40 μM cycloheximide added at time = 0.

Fig. 3 - Effect of proteasomal inhibition on IRP-1 content of mesangial cells. **A)** Quiescent cells in 0.2% serum without additions (Q), or with addition of 10 μg iron/ml (Fe), or iron plus 0.1 μM MG-132 (Fe+MG). **B)** Control cells in 10% serum without additions (C), or with addition of 10 μg iron/ml (Fe), or iron plus 1 μM MG-132 (Fe+MG). In both panels, representative Western blots are shown on top, and mean values ± SD from several independent experiments are represented in the histograms, which show the results of densitometry expressed as a% of control or quiescent cell values taken as 100%. ** Different from Fe alone, $p<0.01$, n=4. * Different from Fe alone, $p<0.05$, n=6.

Fig. 4 - Ubiquitination of IRP-1 in mesangial cells. Quiescent cells in 0.2% serum (panels **A,B**) or control cells growing in 10% serum (panels **C,D**) were either untreated (Q or C) or treated with 10 μg/ml iron for 24 h (Fe) or 0.1 mM DFO for 24 h. In **A)** and **C)**, the pellets from IRP-1 immunoprecipitates were solubilized and subjected to Western blotting with anti-IRP-1 (left side in each panel) or anti-ubiquitin (right side in each panel) antibodies. In **B)** and **D)**, Western blots of IRP-1 and TfR in the corresponding total cell lysates are shown, with β-actin included as a loading control.

Fig. 5 - IRP-1 expression and degradation in LLC-PK1 cells. **A)** Western blots of IRP-1, TfR, and ferritin (Ft) in whole cell lysates of cells grown in control medium (10% serum) with or without 0.1 mM DFO (0+D) for 24 h, or with addition of 1, 5, 10, or 20 μg Fe/ml as FAC for 24 h. β-actin is included as a loading control. **B)** Western blots of IRP-1and β-actin in extracts of cells treated with or without iron (10 μg/ml) in the absence or presence of 1 or 2 μM MG-132 as indicated. **C)** For immunoprecipitation followed by immunblotting (IP/IB), cells were grown without iron, with 10 μg Fe/ml for 24 h, or with 0.1 mM DFO (0+D) for 24 h. Top panel, immunoprecipitate with anti-IRP-1 was blotted with anti-ubiquitin. Second panel, immunoprecipitate with anti-IRP-1 was blotted with anti-IRP-1. Samples in the bottom two panels were not immunoprecipated and cell lysates are blotted for IRP-1 or β-actin.

Fig. 6 - ROS levels following iron chelation or supplementation in LLC-PK1 and mesangial cells. Cells were treated with 0.1 mM DFO (0+D) for 24h without iron supplementation or were supplemented with the indicated concentrations of iron as FAC for 24 h. ROS levels are expressed as mean ± SD compared to the value in cells with no additions taken as 100%. **A)** LLC-PK1 cells, n=4. **B)** RMC cells, n=5. In both panels, differences compared with the control (100%) are indicated as *$p<0.05$, **$p<0.01$.

Fig. 7 - Protein expression in LLC-PK1 cells following silencing of IRP-1 mRNA. siRNA and control experiments were carried out as described in Methods (Section 2.3). Western blots are shown for IRP-1, transferrin receptor (TfR), ferritin (Ft), and β-actin in

extracts of cells that were left untreated, or treated for 24 h with 0.1 mM DFO (0+D), or with the indicated concentration of iron as FAC. The first five lanes are derived from control cells, the next five from silenced cells.

Fig. 8 - Cytosolic aconitase and glutamate levels in LLC-PK1 cells. **A)** Western blotting of IRP-1 was carried out in cytosolic extracts prepared from untreated cells (C) or cells treated with 0.1 mM DFO or supplemented with 10 μg Fe/ml, both for 24 h. Total β-actin and TfR in a membrane fraction are shown for comparison. **B)** Aconitase activity was then measured in these cytosolic extracts and values reported as mean ± SD (n=3 for DFO, n=6 for control and iron). **C)** Glutamate content was measured in the same fractions and reported as mean ± SD (n=7) compared with control taken as 100%. In all cases, significant differences from control values are indicated as *$p<0.05$, **$p<0.01$.

Fig. 9 - Effect of IRP-1 silencing on ROS and glutathione responses in LLC-PK1 cells. **A)** Relative ROS values (mean ± SD, n=5) are compared in untreated cells or cells treated for 24 h with 0.1 mM DFO (0+D) or 10 μg Fe/ml. The first three lanes are from control cells without silencing and the last three lanes are from IRP-1-silenced cells. Bars with the same symbols differ at *$p<0.05$, **$p<0.01$, or ***$p<0.001$. **B)** Cytosolic glutathione levels (mean ± SD, n=6) are measured in the same cells as panel A and expressed relative to the unsilenced/no treatment control taken as 100%. The indicated differences are either not significant (NS) or differ at $p<0.001$ (***).

Fig. 1

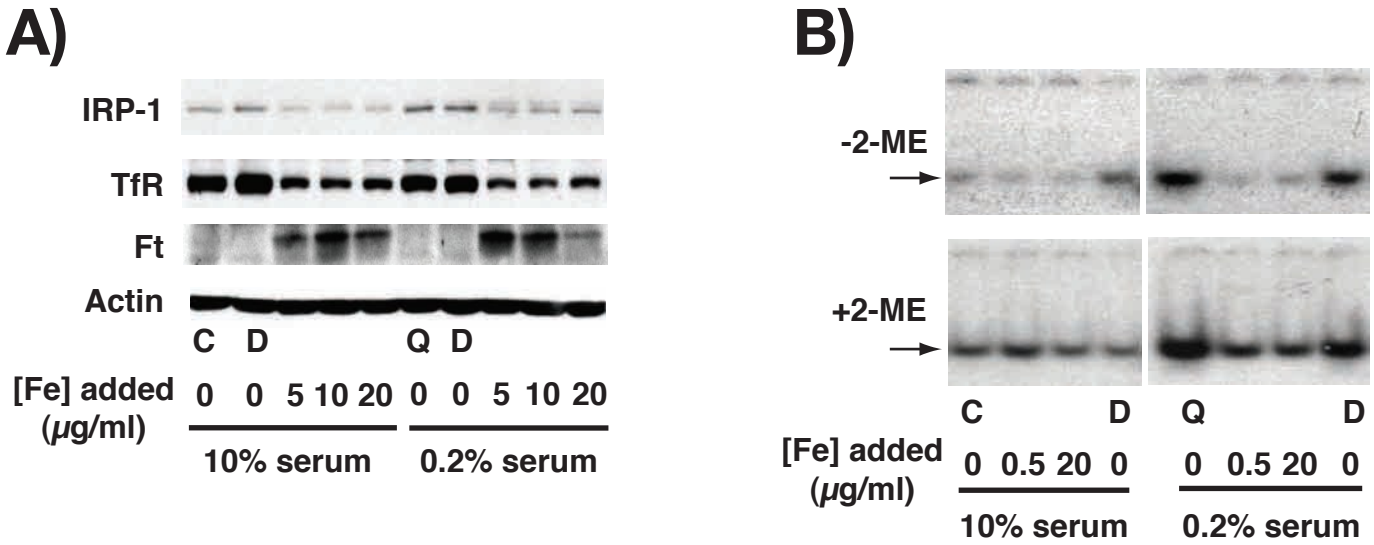

Fig. 2

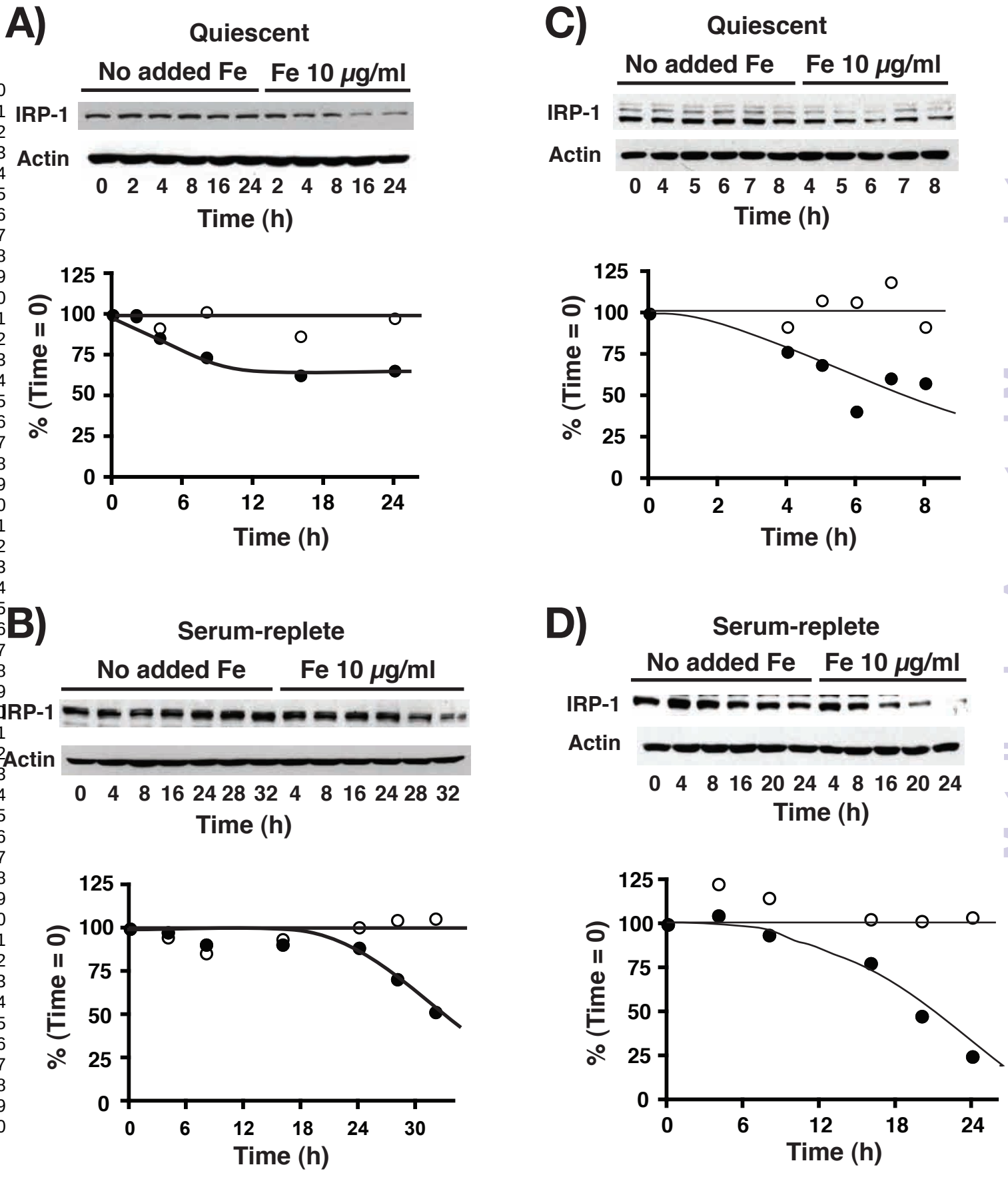

Fig. 3

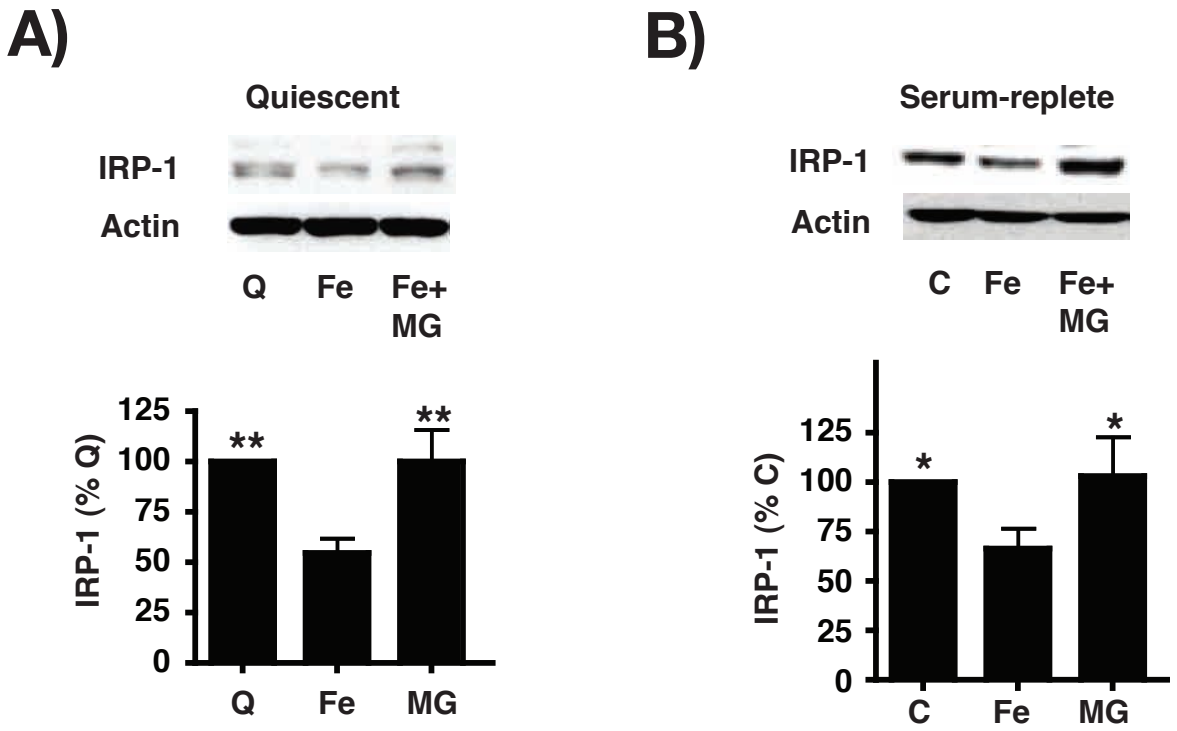

Fig. 4

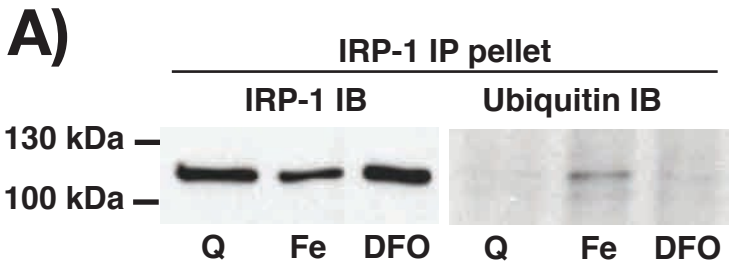

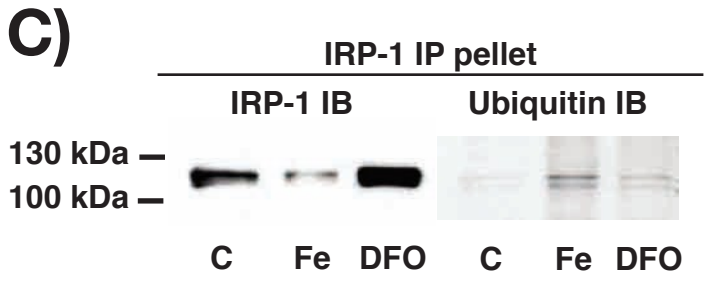

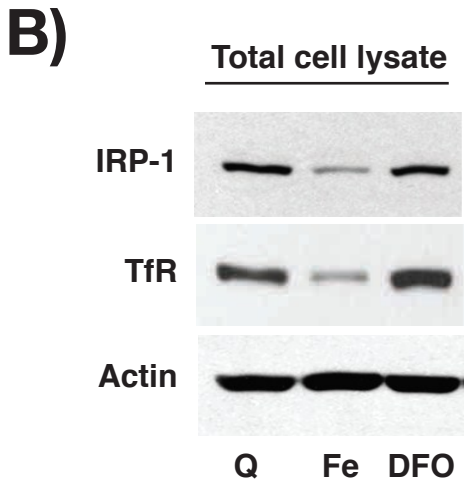

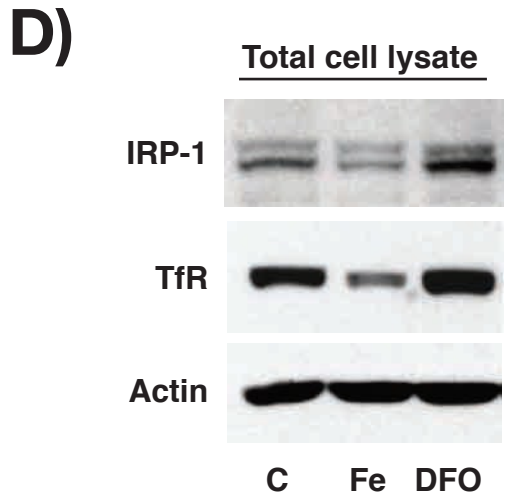

Fig. 5

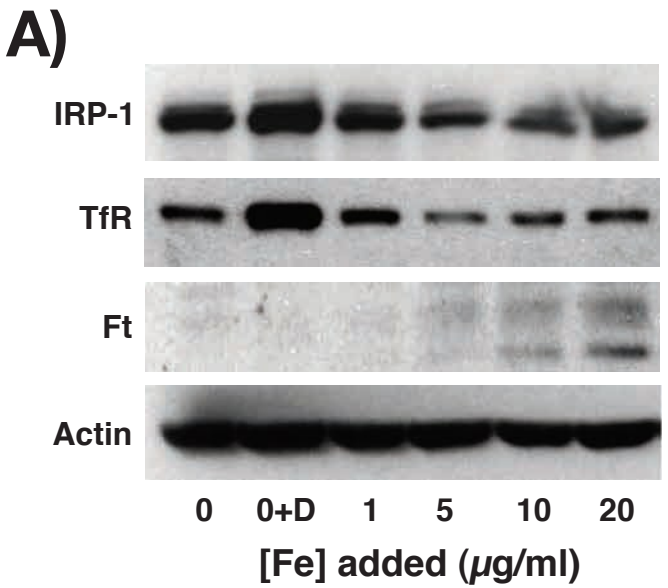

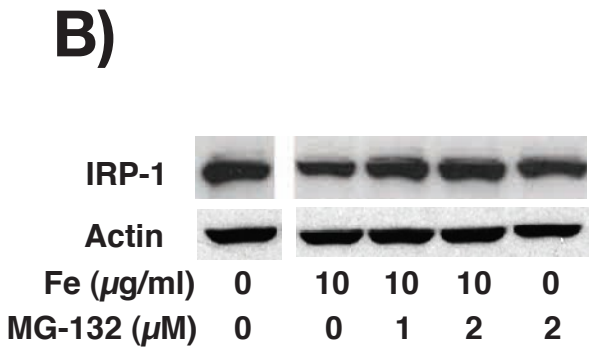

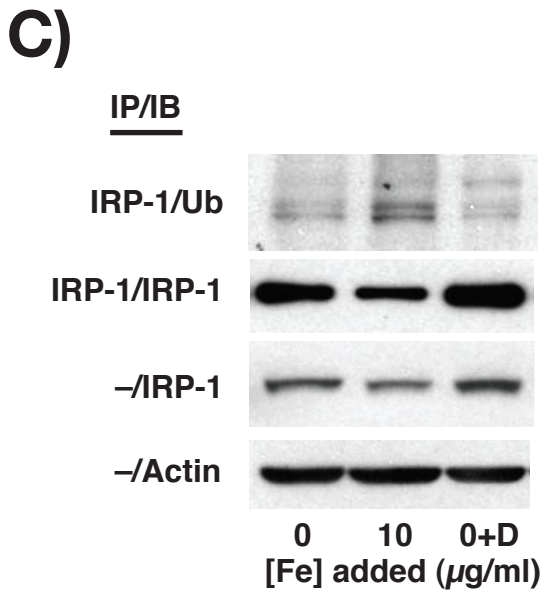

Fig. 6

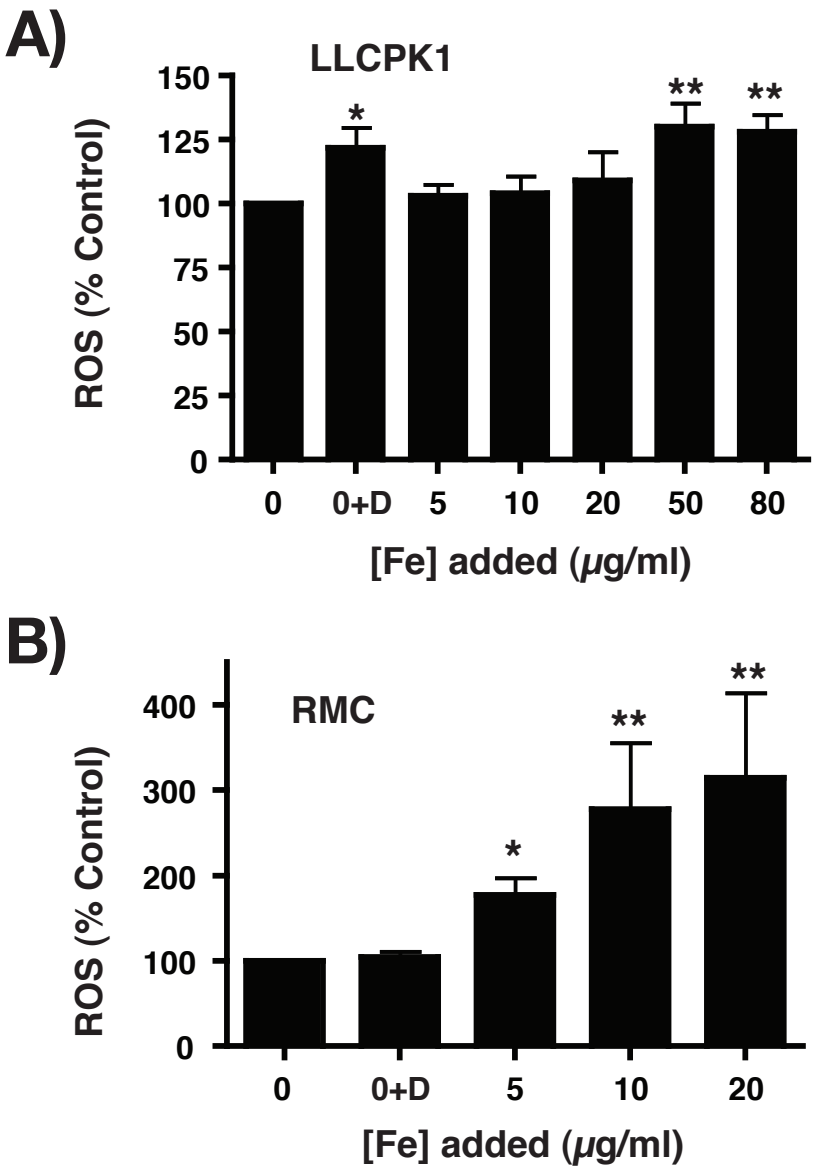

Fig. 7

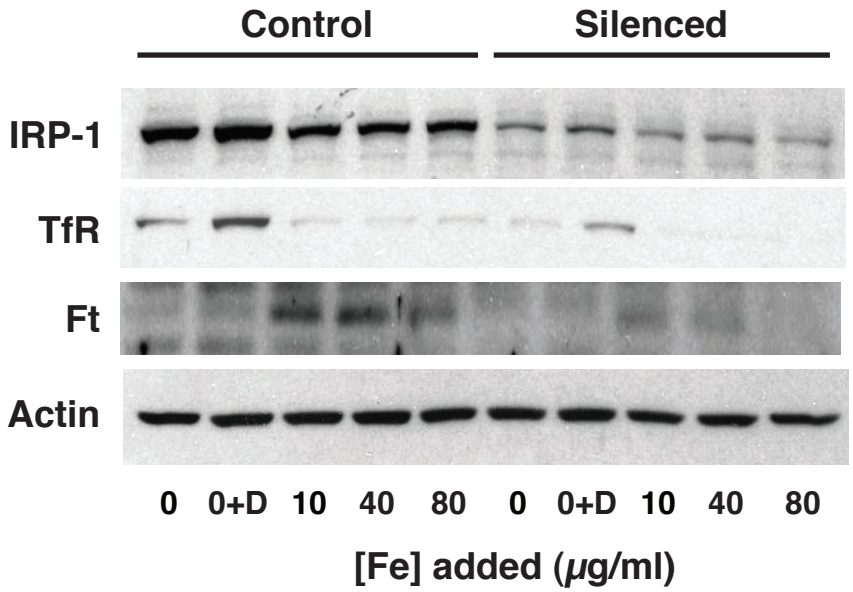

Fig. 8

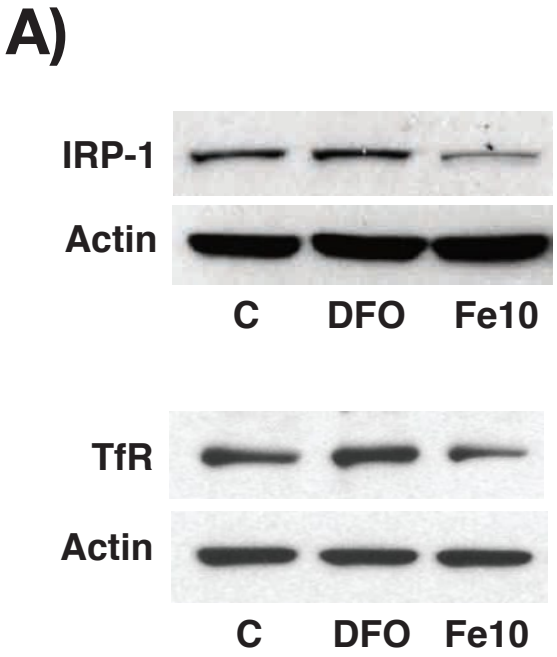

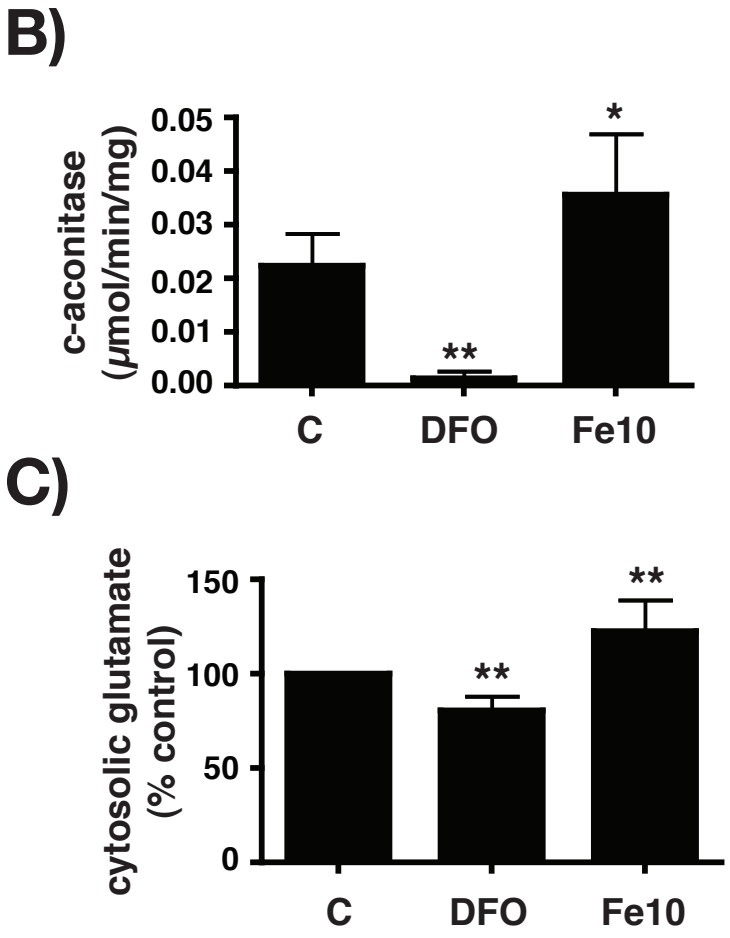

Fig. 9